

The Percolation Theory for High Temperature Superconductors

E. V. L. de Mello, E. S. Caixeiro and J. L. Gonzaléz

Departamento de Física, Universidade Federal Fluminense, av. Litorânia s/n, Niterói, R.J., 24210-340, Brazil

(Received December 2, 2024)

We propose a general theory for the critical T_c and pseudogap T^* temperature dependence on the doping concentration for high- T_c oxides, taking into account the charge inhomogeneities in the CuO_2 planes. The well measured experimental inhomogeneous charge density in a given compound is assumed to produce a spatial distribution of local $\rho(r)$. These differences in the local charge concentration is assumed to yield insulator and metallic regions, possibly in a stripe morphology. In the metallic region, the inhomogeneous charge density yields also spatial distributions of superconducting critical temperatures $T_c(r)$ and zero temperature gap $\Delta_0(r)$. For a given sample, the measured onset of vanishing gap temperature is identified as the pseudogap temperature, that is, T^* , which is the maximum of all $T_c(r)$. Below T^* , due to the distribution of $T_c(r)$'s, there are some superconducting regions surrounded by insulator or metallic medium. The transition to a superconducting state corresponds to the percolation threshold among the superconducting regions with different $T_c(r)$'s. To model the charge inhomogeneities we use a double branched Poisson-Gaussian distribution. To make definite calculations and compare with the experimental results, we derive phase diagrams for the BSCO, LSCO and YBCO families, with a mean field theory for superconductivity using an extended Hubbard Hamiltonian. We show also that this novel approach provides new insights on several experimental features of high- T_c oxides.

Pacs Numbers:74.72.-h, 74.20.-z, 74.80.-g, 71.38.+i

I. INTRODUCTION

It is well known that the properties of high-temperature superconductors (HTSC) vary in an unusual way when a moderate density of holes are introduced into the CuO_2 planes by chemical doping. This is one of the reasons why, despite of a large experimental and theoretical effort, the nature of the superconductivity in these materials remains to be explained¹. Correlations make the parent undoped compound to be a Mott insulator and, upon doping, the underdoped compounds display unusual metallic properties with increasing T_c . Doping beyond the optimal level yields normal metals with Fermi liquid behavior and with decreasing T_c . The non usual properties of underdoped samples have motivated several experiments and two features have been discovered which distinguish them from the overdoped compounds: firstly, the appearance of a pseudogap at a temperature T^* , that is, a discrete structure of the energy spectrum above T_c , identified by several different probes². T^* is found to be present also in overdoped samples^{2,3}, but at temperatures near T_c . Second, there is increasing evidence that the electrical charges are highly inhomogeneous up to (and even further) the optimally doped region⁴⁻⁷. These charge inhomogeneities are not due to impurities but are intrinsic to the type of cuprate, producing local lattice distortions in the CuO_2 bond length⁸. They are also consistent with the presence of charge domains or dynamic charge stripes⁹⁻¹¹.

Therefore, in our view, is very likely that the pseudogap and the intrinsic charge inhomogeneities are intimately related and understanding their connection is of great importance to interpret the general phenomenol-

ogy and the phase diagrams of HTSC. Currently there are two different proposals to explain the existence of the pseudogap, but neither of them deal directly with the intrinsic inhomogeneous charge distribution: In the first, the pseudogap is regarded as a normal state precursor of the superconducting gap due to local dynamic pairing correlations in a state without long range phase coherence, and T_c is much smaller than T^* because of strong phase fluctuations^{12,13}. In the second proposal, the pseudogap is a normal state gap, which is necessarily independent and competing with the superconductivity, existing even below T_c for compounds around the optimum doping, ending in a quantum critical point^{14,15} at zero temperature.

In a recently letter¹⁶ we have proposed a new scenario in which a given cuprate with an average hole per Cu ion density ρ_m and an inhomogeneous microscopic charge distribution produces a distribution of $T_c(r)$. The superconducting transition occurs when the temperature reaches a value which the different superconducting region percolates. The exactly form of the charge inhomogeneities in the CuO_2 planes are not well known but since the discovered of the spin-charge stripes⁹, they are matter of current research. They are well probed by several experiments which demonstrated that the charge distributions are more inhomogeneous for underdoped and more homogeneous for overdoped samples⁴⁻⁷. In the spin-charge stripes scenario, some regions of the plane are heavily doped (the stripes) and other regions are underdoped and fill the space between the charge-rich stripes. Stripes phases occur due to the competition between the antiferromagnetic interaction among magnetic ions and Coulomb interaction between the charges, both

of which favor localization and, on the other hand, the zero-point of the doped holes, which favor delocalization of the charges. Experimentally, the stripes are more easily detected in insulating materials, where they are static, but there is evidence of fluctuating stripe correlations in metallic and superconducting compounds^{10,9,11}.

We therefore use an ansatz to model such charge distributions and assume that it contains two parts: one for a hole-rich and other for a hole-poor partition which mimic the stripes. The hole-poor regions are, in most cases, antiferromagnetic Mott insulators. The hole-rich regions form an inhomogeneous metal with spatially varying charge density. These charge inhomogeneities have several consequences which produces the non-Fermi liquid behavior of these materials. As concerns the superconductivity, they produce spatially dependent superconducting gaps $\Delta_{sc}(r)$ due short coherence length and, superconducting critical temperatures $T_c(r)$. Recent scanning tunneling microscopy data⁷ has measured the spatial variation through the differential conductance which provides an evidence for such distribution of zero temperature superconducting gap $\Delta_{sc}(r)$. Since $T_c(r)$ is proportional to $\Delta_{sc}(r)$, the opening of the largest gap occurs at the highest of all the $T_c(r)$'s, which is exactly T^* . Above T^* there is not any gap and below it, there is the development of some superconducting clusters inside the material. Depending on the distribution of the values of $T_c(r)$ in the compound, some regions become superconducting. Decreasing the temperature, the number of superconducting clusters increases, bringing about the superconducting domains to grow. When the temperature reaches T_c , the superconducting regions percolates through the sample and therefore it can hold a dissipationless current.

This percolating scenario relies largely on the scanning SQUID microscopy magnetic imaging of expel magnetic flux (Meissner effect) domains on LSCO films¹⁷, which shows the regions with the Meissner effect to develop smoothly from around T^* to temperatures well below the percolating threshold T_c , showing the continuous growth of the superconducting region inside the sample as the temperature decreases. We also believe that this experiment cannot be understood neither by the first nor the second scenario. First, the regions without magnetic flux due to the Meissner effect can exist only where the Cooper pairs are in phase coherence. Furthermore there is no apparent difference, other than the size of the superconducting region, as the temperature changes across T_c . Secondly, it shows the existence of the superconducting regions above T_c which differ only in size from those below T_c and therefore goes against a normal state gap competing with the superconductor state. Furthermore, the d-wave nature of both pseudogap and order parameters, the tunneling conductance and ARPES measurements² with their curves evolving smoothly across T_c , are compelling evidences in favor of a similar nature of both gap and pseudogap. Our approach is also supported by the microscopic model based on a spatial dependent critical

temperature $T_c(r)$ due to intrinsic inhomogeneities like pair breakers or spatial dependence of the superconducting coupling constant proposed by Ovchinnikov et al¹⁸. They have derived the density of states due to the spatial distribution of coupling constants.

In this paper we give the details of our previous calculations on Bi2212 family and apply the same methods to the LSCO and YBCO systems. We show that the percolation theory for the HTSC provide good qualitative agreement with T^* and T_c phase diagrams. We have to emphasize that there is a general agreement with respect to the $T_c \times \rho$ curves, since most of them are obtained through the same method, namely, resistivity measurements. However the measured values of T^* found in the literature are obtained through different methods and seems to vary considerably, depending on the specific experimental probe used. Such difference may be due to the anisotropic d-wave nature of the gap amplitude and the fact that a given experimental technique is sensitive to excitations at a particular wavevector magnitude. Therefore, it is natural that angle-resolved photoemission (ARPES), tunneling spectroscopy, transport properties such as dc resistivity and optical conductivity, NMR, Knight shift relaxation rate, electronic Raman, magnetic neutron scattering, specific heat^{2,14} and recent vortex-like Nernst signal measurements¹⁹ yield different values for the onset of vanishing gap temperature T^* .

Our novel scenario not only reproduces the phase diagrams but also provides new physical insight on a number of phenomena detected in the HTSC like: The variation of the pseudogap magnitude with the temperature². The decreasing of the zero temperature superconducting gap Δ_0 while T_c increases for underdoped compounds^{3,20}. The downturn of the linear dependence of the resistivity with the temperature for underdoped samples. The increase of Hall carriers with the temperature, mostly measured for the optimally and underdoped compounds²¹.

This paper is divided as follows: in section II, we discuss the charge distributions and our phenomenological model to mimic the real distribution. In section III, we derive the phase diagram for Bi2212, LSCO and YBCO and make comparison with the experimental data. We use a mean field BCS like method with a extended Hubbard Hamiltonian to derive the onset of vanishing gap, but it should be emphasized that the percolating approach could be worked out with any other method which gives a temperature dependent superconducting gap. In section IV, we comment on the applications and implications of the percolation theory to several physical properties of the HTSC and we finish with the conclusions in section V.

II. THE CHARGE DISTRIBUTION

The consequence of the microscopic charge inhomogeneities distribution in the CuO_2 planes, possibly in a

striped configuration, is the existence of domain walls between the two phases which are spontaneously created in the planes⁹⁻¹¹: regions which are heavily doped or hole-rich may form the stripes and others regions which are hole-poor and are created between the charge-rich stripes. The exactly form of these charge distributions is not known. However, it has been studied by neutron powder diffraction^{5,6,8} on underdoped and optimally doped $La_{2-x}Sr_xCuO_2$. These neutron diffraction experiments suggest that the charge inhomogeneities modifies the $Cu-O$ bond length, leading to a distribution of bond lengths for optimal and underdoped compounds. Scanning tunneling microscopy/spectroscopy⁷ on optimally doped $Bi_2Sr_2CaC_2O_{8+x}$ measure spatial variations in the local density of states and the superconducting gap at a very short length scale of $\approx 14\text{\AA}$.

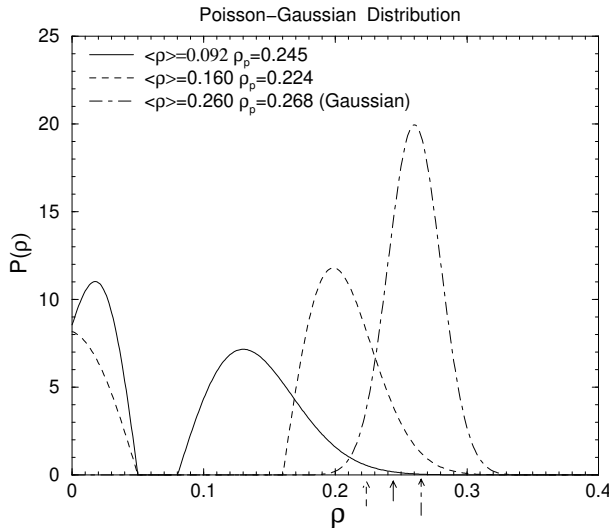


FIG. 1. Model charge distribution for the inhomogeneities or stripe two phase regions. The low density insulating (antiferromagnetic) branch is near $\rho = 0$. The high density hole-rich region starts at the compound average density ρ_m and ρ_p , indicated by the arrows, is the density where percolation can occur.

In order to have a model to the above experimental observations and to be capable of performing calculations which may reproduce the measured phase diagrams, we use a combination of a Poisson and a Gaussian distribution. This combination was chosen because each distribution has a convenient property which we used below: The width of a Gaussian distribution is easy to be controlled and expresses the degree of disorder but since it is symmetric, it is difficult to apply to the low density compounds. The Poisson distribution starts sharply and has a long tail which is convenient to these low densities compounds with their large degree of inhomogeneities. For a given compound with an average charge density ρ_m , the hole distribution $P(\rho; \rho_m)$ is a function of the local hole density ρ , separated in two branches or domains. The low density branch represents the hole-poor or non-

conducting regions and the high density one represents the hole-rich or metallic regions. As concerns the superconductivity, only the properties of the hole rich branch are important since the currents flow only through the metallic region.

Such distribution may be given by:

$$P(\rho) = (\rho_c - \rho) \exp[-(\rho - \rho_c)^2/2(\sigma_-)^2] / [(\sigma_-)^2(2 - \exp[-(\rho_c)^2/2(\sigma_-)^2])] \quad \text{for } 0 < \rho < \rho_c \quad (1)$$

$$P(\rho) = 0 \quad \text{for } \rho_c < \rho < \rho_m \quad (2)$$

$$P(\rho) = (\rho - \rho_m) \exp[-(\rho - \rho_m)^2/2(\sigma_+)^2] / [(\sigma_+)^2(2 - \exp[-(\rho_c)^2/2(\sigma_-)^2])] \quad \text{for } \rho_m < \rho \quad (3)$$

The values of σ_{\pm} controls the width of the low (-) and the high (+) density branch. As the doping level increases, we take larger values of σ_- and smaller values of the metallic branch width σ_+ . $\rho_c \approx 0.05$ is taking as the end of the low branch because it corresponds to the onset of superconductivity to mostly cuprates. However, $\rho_c \approx 0.1$ for Bi2212. ρ_m is the approximate hole density of a given compound. The density distribution is normalized to unity. For densities of $\rho > 0.25$, that is, in the far overdoped region, we use a single Gaussian distribution which reflects the more homogeneous character of these compounds.

A compound having regions with different hole concentration which are distributed according to our density function $P(\rho)$, has an average value which depend on the parameters of the distribution. We can show that the average value of our density distribution is

$$\langle \rho \rangle = [\sigma_+ \text{sqrt}(\pi/2) + \rho_m + \rho_c - \sigma_- \text{sqrt}(\pi/2) \times \text{erfunction}(\rho_c/\text{sqrt}(\pi/2))] / [(\sigma_+)^2(2 - \exp[-(\rho_c)^2/2(\sigma_-)^2])]. \quad (4)$$

here erf function is the error function. For most compounds, due to the small values of σ_+ , $\langle \rho \rangle \approx \rho_m$, see Table I below. Indeed, for a compound with average density ρ_m , the values of σ_{\pm} are chosen in order that percolation in the hole-rich branch occurs exactly at a given density ρ_p .

ρ_m	σ_-	σ_+	$\langle \rho \rangle$	ρ_p
0.080*	0.033	0.050	0.09	0.245
0.100	0.034	0.050	0.10	0.240
0.120	0.037	0.050	0.12	0.238
0.160*	0.057	0.037	0.16	0.225
0.200	0.078	0.026	0.20	0.239
0.220	0.090	0.024	0.22	0.245
0.260*	0.04(G)	0.04(G)	0.26	0.268

TABLE I. Some selected parameters for different doping level compounds. Notice that they are characterized by the average hole density ρ_m given in the first column. Notice also that the values of the metallic branch width σ_+ decreases with ρ_m , showing that the degree of disorder decrease with the doping. The * marks the distributions plotted in Fig.1

In the next section we show how to estimate T_c as function of ρ , that is $T_c(\rho)$. Thus $T^*(\rho_p)$ is the maximum temperature which the system can percolate and which we identify as equal to $T_c(\rho_m)$.

According to percolation theory, the percolation threshold occurs in a square lattice when 59% of the sites or bonds are filled²². Thus, we find the density where the hole-rich branch percolates integrating $\int P(\rho)d\rho$ from ρ_m till the integral reaches the value of 0.59, where we define ρ_p . Below $T_c(\rho_m)$ the system percolates and, consequently, it is able to hold a dissipationless supercurrent. In the Table I, we show some of the parameters used for certain sample and we plot the distribution, as discussed above, in Fig.1. Notice that the table and figure are for HTSC with optimum doping $\rho_m \approx 0.16$ like LSCO or YBCO. For Bi2212, the optimum hole doping is about the double²³ and in this case new parameters must be used. Some distributions used for the calculations with the Bi2212 family, similar to Fig.1 above, was published before¹⁶.

III. THE PHASE DIAGRAM

In this section we need a method which yields a superconducting critical temperature as function of the density of carriers to be used in connection with the distributions given in the previous section. For simplicity we will follow a BCS-like approach with an extended Hubbard Hamiltonian to derive a curve for the temperature onset of vanishing gap T^* as function of the hole concentration ρ_m . This approach, with appropriate choice of experimental or calculated parameters, was used before to derive the $T_c \times \rho$ curves^{24–26} for some HTSC family, since T_c was, as in normal superconductors, taken as the onset of vanishing gap. A two dimension extended Hubbard Hamiltonian in a square lattice has been used to model the quasi-bidimensionality of the motion of the charge carriers through the CuO_2 planes^{24–26,28} and is given by

$$H = - \sum_{\ll ij \gg \sigma} t_{ij} c_{i\sigma}^\dagger c_{j\sigma} + U \sum_i n_{i\uparrow} n_{i\downarrow} + \sum_{\langle ij \rangle \sigma \sigma'} V_{ij} c_{i\sigma}^\dagger c_{j\sigma'}^\dagger c_{j\sigma'} c_{i\sigma}, \quad (5)$$

where t_{ij} is the nearest-neighbor and next-nearest-neighbor hopping integral between sites i and j ; U is the Coulomb on-site correlated repulsion and V_{ij} is the attractive interaction between nearest-neighbor sites i and j . a is the lattice parameter.

Using the well known BCS-type mean-field approximation to develop Eq.(5) in the momentum space, one obtains the self-consistent gap equation, at finite temperatures²⁷

$$\Delta_{\mathbf{k}} = - \sum_{\mathbf{k}'} V_{\mathbf{kk}'} \frac{\Delta_{\mathbf{k}'}}{2E_{\mathbf{k}'}} \tanh \frac{E_{\mathbf{k}'}}{2k_B T}, \quad (6)$$

with

$$E_{\mathbf{k}} = \sqrt{\varepsilon_{\mathbf{k}}^2 + \Delta_{\mathbf{k}}^2}, \quad (7)$$

which contains the dispersion relation $\varepsilon_{\mathbf{k}}$, and the interaction potential $V_{\mathbf{kk}'}$ which comes from the transformation to the momentum space of Eq.(5)^{24,28}. In the calculations we have used a dispersion relation derived from the ARPES data²⁹ with five neighbors hopping integrals. The hopping integrals could also be estimated from band structure calculations³⁰. The interaction potential may be given by^{24,28}.

$$V_{\mathbf{kk}'} = U + 2V \cos(k_x a) \cos(k'_x a) + 2V \cos(k_y a) \cos(k'_y a). \quad (8)$$

The substitution of Eq.(8) into Eq.(6) leads to appearance of a gap with two distinct symmetries²⁴:

$$\Delta_{\mathbf{k}}(T) = \Delta(T) [\cos(k_x a) \pm \cos(k_y a)], \quad (9)$$

where the plus sign is for extended- s wave and the minus sign, for d wave symmetry. In accordance with Ref²⁴ one observes that the d wave part of the gap do not depend on the coupling constant U , depending only on V . Here we deal only with the d -wave which is the more accepted pseudogap symmetry².

Using the same BCS-type mean-field approximation, one obtains the hole-content equation³¹

$$\rho(\mu, T) = \frac{1}{2} \sum_{\mathbf{k}} \left(1 - \frac{\varepsilon_{\mathbf{k}}}{E_{\mathbf{k}}} \tanh \frac{E_{\mathbf{k}}}{2k_B T} \right), \quad (10)$$

where $0 \leq \rho \leq 1$.

Eq.(10) together with the gap equation (6) must be solved together self-consistently. They may be used to derive the onset of vanishing gap temperature as function of the density of carriers ρ . This procedure was used in the past to derive, with appropriate set of parameters, the $T_c \times \rho$ phase diagram for different HTSC systems for a single type^{24,25,28,32} and for mixture of different order parameter symmetry³³. In the present work, we assume a different view. We take the onset of vanishing gap temperature as the pseudogap temperature T^* and derive the $T^* \times \rho$ phase diagram for the $La_{2-x}Sr_xCuO_4$ and $YBa_2Cu_3O_x$ series of superconductors. The change between T_c and T^* can be achieved with small changes in the hopping parameters and an increase in the attractive potential, which is the free parameter of this type of calculation.

Below, in Fig.2, we present the results for the $La_{2-x}Sr_xCuO_4$ family. We have used a dispersion relation derived from the Schabel et al²⁹. The hopping parameters are: $t_1=0.35\text{eV}$, $t_2/t_1=0.55$, $t_3/t_1=0.29$, $t_4/t_1=0.19$, $t_5/t_1=0.06$. The magnitude of the attractive potential was set $V/t=-0.40$ in order to give a reasonable agreement with many measured values of T^* . As

we have already mentioned, different experiments yield completely different results for T^* . Varying V/t makes the $T^* \times \rho$ curve to go up or down, but does not change the position of the optimal density. These hopping values are within the variation estimated by different methods (band structure, ARPES measurement, etc.), which results in different values^{34,35}. The $T^* \times \rho$ curve is in good qualitative agreement with the displayed experimental data^{19,36}.

The theoretical curves in Fig.2 are derived in the following way. A given sample with average density ρ_m has its T^* given by the value $T^*(\rho_m)$ derived from the calculated $T^* \times \rho$ curve. The value of T_c is estimated in the following manner: for the compound of density ρ_m , according to the previous section, we calculate the value where percolation occurs in the metallic branch which starts at ρ_m , that is, ρ_p . The associated $T^*(\rho_p)$ is the maximum percolating temperature, that is $T_c(\rho_m) \equiv T^*(\rho_p)$. We have also used this procedure to calculate the phase diagram for the Bi2212 family which is in agreement with the experimental data¹⁶ and below we show the results for the LSCO family. A similar curve was also studied which the T^* is in reasonable agreement with the T_c^{MF} extracted from the high-resolution dilatometry data³⁷ for $YBa_2Cu_3O_x$.

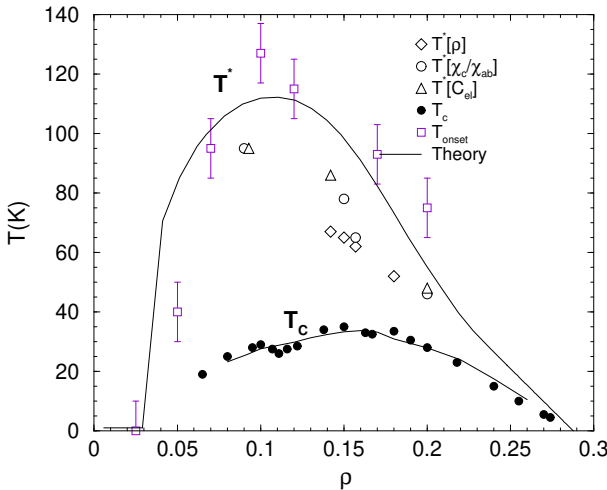


FIG. 2. Phase diagram for the onset of vanishing gap temperature T^* vs. ρ with d wave symmetry. The experimental data are taken from Ref.³⁶ and T_{onset} is taken from the flux flow experiment of Ref.¹⁹ (open squares).

IV. DISCUSSION

There are several experimental observations and measurements on the HTSC, besides the data for the phase diagram discussed above, that can be well explained with the percolating approach. We will discuss here some examples.

The fact that all experiments show that T^* is a monotonically decreasing function of ρ for the metallic com-

pounds, as seen in Fig.2 for $\rho \geq 0.1$ is very suggestive. In our view, T^* marks the onset of vanishing superconducting gap, it means that the superconducting transition temperature decreases upon doping. However the materials become good metals since, as the doping level increases, the compounds change from very poor metals in the normal phase to very good metals with typical Fermi liquid behavior in the overdoped region. This may be taken as an evidence of a superconducting interaction mediated by phonons, as it is well known that materials whose vibrating atoms interact strongly with the electrons, and are poor metals, should become superconductors at higher temperatures than those good metals, whose atoms interact weakly with electrons³⁹. Notice that this is a pure experimental fact independent of our calculations if one assumes T^* as the onset of vanishing superconducting gap.

However there are other implications of our model and calculations:

i-ARPES measurements^{3,20} have revealed the anomalous behavior of the zero temperature gap $\Delta_0(\rho_m)$ which decreases steadily with the doping ρ_m although T_c increases by a factor of 2 for their underdoped samples. In the overdoped region, since T_c also decreases, the behavior is the expected conventional proportionality. This overall relation between $\Delta_0(\rho_m)$ and T_c is totally unexpected since it is well known that normal superconductors have a constant value for the ratio $2\Delta_0/k_B T_c$, being 3.75 for usual isotropic order parameter and 4.18 for $d_{x^2-y^2}$ wave solution³⁸.

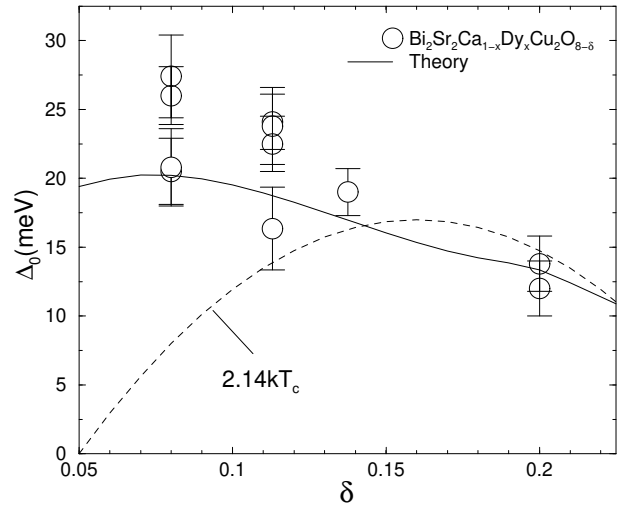


FIG. 3. The zero temperature gap for 9 samples as measured by Harris et al²⁰ and our calculations.

At low temperatures, since the superconducting phase percolates through different regions, each one possesses a given $\Delta_0(r)$, tunneling and ARPES experiments detect the largest gap present in the compound. Consequently, $\Delta_0(\rho_m)$ must be correlated with the onset of vanishing gap $T^*(\rho_m)$ which is the largest superconducting temper-

ature in the sample, and should not be correlated with $T_c(\rho_m)$. As we show in Fig.3, correlating the values plotted in Fig.2 for $T^*(\rho_m)$ with $\Delta_0(\rho_m)$, we are able to give a reasonable fit for the data^{3,20} on $Dy-BSCCO$ and explains the different energy scales pointed out by several others authors.

ii-Transport experiments have also been used to study the pseudogap². The underdoped and optimum doped high- T_c oxides have a linear behavior for the resistivity in the normal phase up to very high temperatures. However, at T^* there is a deviation from the linear behavior and the resistivity falls faster with decreasing temperature^{2,36}. This behavior can be understood by the increasing of superconducting cluster numbers and size, as the temperatures decreases below T^* . Each superconducting cluster produces a short circuit which decreases the resistivity below the linear behavior between T^* and T_c . To obtain a quantitative fitting of this effect, we are presently working on a simulation for the resistivity of a linear metallic medium with short circuited regions which varies with the temperature.

iii-Several measurements made in the presence of a magnetic field seem to agree with the percolating scenario: The increase of the resistivity in a $La_{2-x}Sr_xCuO_4$ film just above the irreversibility line measured by magnetotransport⁴¹ is in agreement with the notion that the magnetic field penetrates partially in the superconducting regions and destroys some of the superconducting clusters in the film. We have already mentioned the recent measurements of magnetic domains above T_c which has been interpreted as a diamagnetic precursor to the Meissner state, produced by performed pairs in underdoped $La_{2-x}Sr_xCuO_4$ thin films¹⁷. The existence of superconducting clusters between T^* and T_c easily explains the appearance of local diamagnetic or Meissner domains and, if there is a temperature gradient in the sample, the local flux flows and produces the dynamic flux flow state¹⁹.

iv-Another important consequence which follows, is that the superconducting pairing mechanism should be more easily investigated by experiments performed mainly at T^* . A such experiment was accomplished by Rubio Temprano et al⁴², which measured a large isotope effect associated with T^* and an almost negligible isotopic effect associated with T_c in the slightly underdoped $HoBa_2Cu_4O_8$ compound. The results strongly support the fact that electron-phonon induced effects are present in the superconducting mechanism associated with T^* . Bussmann-Holder et al have also calculated T^* as function of a phonon induced gap⁴³.

In order to gain further insight on the nature of the pair potential, we have measured the resistivity under hydrostatic pressure on an optimally doped $Hg_{0.82}Re_{0.18}Ba_2Ca_2Cu_3O_{8+\delta}$ ⁴⁴ sample. The data indicate a linear increase of T^* with the pressure at the same rate as T_c . In the context of our theory, this result also supports the phonon induced mechanism: the inhomogeneities local charge densities in a given compound yield

varying values for the Fermi level, broadening $N(E_F)$ ¹⁸. The applied pressure on a cuprate with an inhomogeneous charge distribution is also expected to broaden the density of states²⁴ $N(E_F)$, and the main effect of an applied pressure on T_c is an increase of the phonon or Debye frequency. This is seen through the linear increase of T^* ⁴⁴ which also provides a very interesting physical explanation on the origin of the linear pressure induced *intrinsic effect*^{24,45,46}, usually postulated to explain the raise of T_c above its maximum value.

v-Another anomalous behavior found mostly in underdoped compounds is related with the temperature behavior of the Hall coefficient²¹ R_H and the Hall density n_H which is proportional to the average hole density $\langle \rho \rangle$. While in normal metals n_H is independent of the temperature, in the normal phase of many HTSC, n_H increases monotonically as the temperature increases and saturates at high temperatures^{21,40}. This anomalous behavior can be explained by the existence of superconducting islands above T_c which gradually turn into metallic phase as the temperature is raised. Such superconducting regions can be regarded as empty spaces in a disordered hole-rich (metallic) and hole-poor (insulator) background. Therefore, as the metallic region increases, it increases also the number of carrier. However, we have to point out that the saturation seems to occur near the room temperature, which is much higher than some of the measured values for T^* .

V. CONCLUSIONS

We have proposed a novel and general approach to the phase diagram of the high- T_c cuprates superconductors in which the pseudogap is the largest superconducting gap among the superconducting regions in an inhomogeneous compound and the critical temperature T_c is the maximum temperature for which these superconducting regions percolate. We have shown, through the calculations presented in this paper, that this approach is suitable to reproduce the measured T_c and T^* phase diagrams for several cuprates, which includes many different type of data. Although we have used a mean field BCS like method to obtain the superconducting gap, these calculations could had been done with other superconducting approaches. This new general approach is, to our knowledge, the only method which is able to calculate such phase diagrams taking into account the well known charge inhomogeneities of HTSC. However, since the exact charge distribution has not yet been determined, we had to use a stripe like ansatz for such distributions.

Our novel method provides new insights and introduces a new interpretation or new scenario to the existence of the pseudogap and T^* . We have also shown that the percolating approach has several implications on several typical anomalous properties of HTSC like the dependence of the zero temperature gap $\Delta_0(T)$ with the

hole concentration, the downturn of the linear dependence to the resistivity with the temperature, the linear dependence of the hole concentration with the temperature, dependence of T^* with the pressure, and others new implications which are presently being studied and which will be discussed in further publications.

Financial support of CNPq and FAPERJ is gratefully acknowledged. JLG thanks CLAF for a CLAF/CNPq pos-doctoral fellowship.

¹ K. Kitazawa, Proceedings of the IV-M2S HTSC conference, *Physica C* **341-348**, 19 (2000).

² T. Timusk and B. Statt, *Rep. Prog. Phys.*, **62**, 61 (1999).

³ C. Renner, B. Revaz, J.-Y Genoud, K. Kadowaki, and O. Fischer, *Phys. Rev. Lett.* **80**, 149 (1998).

⁴ T. Egami and S.J.L. Billinge, in "Physical Properties of High-Temperatures Superconductors V" edited by D.M. Greensberg, World Scientific, Singapore 1996), p. 265.

⁵ S.J.L. Billinge, J. Supercond., Proceedings of the Conf. "Major Trends in Superconductivity in New Milenium", 2000.

⁶ E.S. Bozin, G.H. Kwei, H. Takagi, and S.J.L. Billinge, *Phys. Rev. Lett.* **84**, 5856, (2000).

⁷ S. H. Pan, J. P. O'Neal, R. L. Badzey, C. Chamon, H. Ding, J. R. Engelbrecht, Z. Wang, H. Eisaki, S. Uchida, A.K. Gupta, K. W. Ng, E. W. Hudson, K. M. Lang, J. C. Davis *Nature*, **413**, 282-285 (2001) and cond-mat/0107347.

⁸ T. Egami, Proc. of the New3SC International Conference, *Physica C* **364-365**, (2001).

⁹ J.M.Traquada, B.J. Sternlieb, J.D. Axe, Y. Nakamura, and S. Uchida, *Nature (London)*, **375**, 561 (1995).

¹⁰ A. Bianconi, N.L. Saini, A. Lanzara, M. Missori, T. Rossetti, H. Oyanagi, Y. Yamaguchi, K. Oda and T. Ito, *Phys. Rev. Lett.* **76**, 3412 (1996).

¹¹ V.J. Emery, S.A. Kivelson and J.M.Traquada, Proc. Natl. Acad. Sci. USA **96**, 8814 (1999).

¹² M. Randeria, cond-mat/9710223.

¹³ V.J. Emery and S.A. Kivelson, *Nature (London)*, **374**, 434 (1995).

¹⁴ J.L. Tallon and J.W. Loram, *Physica C* **349**, 53 (2001).

¹⁵ G.V.M. Williams, J.L. Tallon, J.W. Quilty, H.J. Trodahl, N.E. Flower, *Phys. Rev. Lett.* **80**, 377 (1998).

¹⁶ E.V.L. de Mello, E.S. Caixeiro and J.L. Gonzalez, submitted to publication, cond-mat/0110479.

¹⁷ I. Iguchi, I. Yamaguchi, and A. Sugimoto, *Nature*, **412**, 420 (2001).

¹⁸ Yu.N. Ovchinnikov, S.A. Wolf, V.Z. Kresin, *Phys. Rev. B* **63**, 064524, (2001), and *Physica C* **341-348**, 103, (2000).

¹⁹ Z.A. Xu, N.P. Ong, Y. Wang, T. Kakeshita, and S. Uchida, *Nature* **406**, 486 (2000) and cond-mat/0108242.

²⁰ J.M Harris, Z.X. Shen, P.J. White, D.S. Marshall, M.C. Schabel, J.N. Eckstein, and I. Bozovic, *Phys.Rev. B* **54** R15665 (1996).

²¹ N.P. Ong, "Physical Properties of High Temperature Superconductors", Vol. II, ed. D.M. Ginsberg, (Singapore, World Scientific) 459, (1990).

²² D.F. Stauffer and A. Aharony, "Introduction to Percolation Theory". Taylor&Francis Ed., London, 1994.

²³ P. Konsin, N. Kristoffel, and B. Sorkin, *J. Phys. C.M.* **10**, 6533 (1998).

²⁴ G.G.N. Angilella, R. Pucci, and F. Siringo, *Phys. Rev. B* **54**, 15471 (1996).

²⁵ E. V. L. de Mello, *Physica C* **259**, 109 (1996).

²⁶ E. V. L. de Mello, *Braz. J. Phys.* **29**, 551 (1999), and *Physica B* **265**, 142 (1999).

²⁷ P. G. de Gennes, *Superconductivity of Metals and Alloys*, W. A. Benjamin, New York, 1966.

²⁸ T. Schneider and M. P. Sørensen, *Z. Phys. B* **80**, 331 (1990).

²⁹ M. C. Schabel, C. -H. Park, A. Matsuura, Z.-X. Shen, D.A. Bonn, X. Liang, W.N. Hardy, *Phys. Rev. B* **57**, 6090 (1998).

³⁰ M. S. Hybertsen, M. Schluter, and N. E. Christensen, *Phys. Rev. B* **39**, 9028 (1989).

³¹ A. J. Leggett, *Rev. Mod. Phys.* **47**, 331 (1975).

³² E. S. Caixeiro, and E. V. de Mello, *Physica C* **353**, 103 (2001).

³³ E. V. de Mello, *Physica C* **324**, 88 (1999).

³⁴ R. Raimondi, J. H. Jefferson, and L.F. Feiner, *Phys. Rev. B* **53**, 8774 (1996).

³⁵ O. K. Andersen, A. I. Liechtenstein, O. Jepsen, and F. Paulsen, *J. Phys. Chem. Solids*, Vol.56, No.12, pp. 1573-1591 (1995).

³⁶ M. Oda, N. Momono, and M. Ido, *Supercond. Sci. Technol.* **13**, R139 (2000).

³⁷ C. Meingast, V. Pasler, P. Nagel, A. Rykov, S. Tajima, and P. Olsson, *Phys.Rev.Lett* **86** 1606 (2001).

³⁸ H. Won and K. Maki, *Phys. Rev. B* **49**, 1397 (1994).

³⁹ B.T. Matthias, "Superconductivity", *Scientific American*, 92, November of 1957.

⁴⁰ Y. Wang, and N.P. Ong, cond-mat/0110215.

⁴¹ B. Lake et al, *Science*, **291** 1759 (2001), cond-mat/0104026.

⁴² D. Rubio Temprano, J. Mesot, S. Janssen, K. Conder, A. Furrer, H. Mutka, and K.A. Muller, *Phys.Rev.Lett* **84**, 1990 (2000).

⁴³ A. Bussmann-Holder, Alan R. Bishop, H. Büttner, T. Egami, R. Micnas, and K.A. Müller, *J.Phys. C.M.* **13**, L169, (2001).

⁴⁴ E.V.L. de Mello, M.T.D. Orlando, E.S. Caixeiro, J.L. González, and E. Baggio-Saitovitch, submitted to publication, cond-mat/0110462.

⁴⁵ M.T.D. Orlando, A.G Cunha, E.V.L. de Mello, H.Belich, E. Baggio-Saitovitch, A. Sin, X. Obradors, T. Burghardt, A. Eichler, *Phys. Rev. B* **61**, 15454 (2000).

⁴⁶ J.L. Gonzalez, E.S. Yague, E. Baggio-Saitovitch, M.T.D. Orlando, and E.V.L. de Mello, *Phys. Rev. B* **63**, 54516 (2001).